BILINGUAL PUBLISHING GROUP

Journal of Atmospheric Science Research

https://journals.bilpubgroup.com/index.php/jasr

ARTICLE

A Mathematical Model for Fluxes Associated with Airflow over Northeast Region of India

Prasanta Das

Department of Mathematics, Ramananda College, Bankura 722122, India

ABSTRACT

An attempt has been made to study the horizontal momentum flux and vertical energy flux associated with baroclinic airflow over northeast region of India. The northeast region of India features two prominent orographic barriers: the Assam-Burma Hills (ABH) and the Khasi-Jaintia Hills (KJH). This paper presents a three-dimensional (3-D) model for mountain waves, applied to calculate momentum flux (MF) and energy flux (EF) associated with airflow over the Assam-Burma Hills (ABH) and Khasi-Jaintia Hills (KJH) in northeast India. We investigate the impact of the Assam-Burma Hills (ABH) and Khasi-Jaintia Hills (KJH) on momentum flux and energy flux associated with vertically propagating internal gravity waves, considering a realistic airflow with height-dependent wind and stability profiles. The model employs a comprehensive set of assumptions, including a three-dimensional (3D) laminar flow regime, inviscid fluid behavior, adiabatic conditions, and the Boussinesq approximation, all within the context of a non-rotating moist airflow environment. The simulation yields detailed results for the energy flux along the vertical z-axis, as well as the two horizontal components of momentum flux along the x-axis and y-axis. These results have been thoroughly evaluated and subsequently compared with the findings of earlier researchers in the field, facilitating a robust validation of the model's performance.

Keywords: ABH; KJH; MF; EF

*CORRESPONDING AUTHOR:

Prasanta Das, Department of Mathematics, Ramananda College, Bankura 722122, India; Email: pdas.math1986@gmail.com

ARTICLE INFO

Received: 5 May 2025 | Revised: 15 June 2025 | Accepted: 22 June 2025 | Published Online: 17 July 2025
DOI:https://doi.org/10.30564/jasr.v8i3.10177

CITATION

Das. P., 2025. A Mathematical Model for Fluxes Associated with Airflow over Northeast Region of India.Journal of Atmospheric Science Research.8(3): 24–35.DOI:https://doi.org/10.30564/jasr.v8i3.10177

1. Introduction

When a stably stratified air-stream flows across an orographic barrier, the gravity waves occur and it can transport the momentum from stably tabular air stream to the ground surface in response to a net pressure drop between the windward and lee slopes of the barrier. Also, these type of gravity waves able to carry energy from ground surface to the mean flow at great height. It is also known that the breaking of gravity waves leading to turbulence may be due to continuous extraction of momentum from the mean flow. The transport of energy and momentum associated by gravity waves is a sub-grid scale phenomenon. So, the parameterization of these sub-grid scale fluxes (energy flux and momentum flux) is very significant in the NWP (Numeric Weather Prediction) models. Numerous researchers have theoretically studied stably stratified airflow across various orographic barriers.

Corby and Sawyar (1958)[1] studied the effects of the upper boundary and high level conditions over a ridge. They showed that lee waves may reach their maximum amplitude in the high troposphere and stratosphere of some airstreams. The properties of these waves are mostly determined by the nature of the airstream at high altitudes, although the more well-known kind of lee wave, which has its maximum amplitude in the lower troposphere, is seldom affected. Sawyar (1959)[2] studied the effects of topography into methods of numerical forecasting. He considered a two-dimensional (2-D) bell-shaped obstacle and obtained a typical value of momentum flux of magnitude 1–10dynes/cm^2. He also observed that the impact of topographic features be integrated into models serving as the foundation for numerical weather prediction, to the extent feasible. Nevertheless, the dynamic processes through which hills and mountains affect large-scale weather systems remain incompletely comprehended. He reviewed the likely mechanisms involved, assessed their significance, and proposed adaptations to the quasigeostrophic models used in numerical forecasting.

Eliaseen (1961)[3] also taken a 2-D flux model for a steady and non-dissipative waves. He observed that the horizontal momentum flux is independent of height. For a steady, non-rotating, 3-D linear problem, the governing equation becomes nonsingular when the environmental flow velocity is normal to a given wave number vector, as shown by Sawyar (1962)[4]. Bluemen (1965)[5] developed a random model of momentum flux by mountain waves. He showed that the maximum value of flux is attend when the vertical wavelength is two times of height of the mountain. Booker and Bretherton (1967)[6] observed a critical layer where momentum flux is absorbed and environmental wind speed vanishes when Richardson number is more than 0.25.

Miles (1968)[7] studied about drag and wave amplitude for a 2-D thin barrier. He observed that wave drag tends to increase when decreasing wind speed. He also showed that the wave amplitudes and drag for a thin barrier in a two dimensional stratified flow in which the dynamic pressure and density gradient of the upstream wind are constants. Bretherton (1969)[8] viewed that the momentum transfer from the waves to the mean flow during propagation. In the review he judged that an upward transport of horizontal momentum inevitably accompanies the generation of such waves in he atmosphere, the mean flow being affected only precisely at those levels, where the waves are dissipated. He had also shown that if the mean wind depends on the horizontal position, there might be a continuous transfer of momentum from the waves to the mean flow during propagation. In the absence of intense clear air turbulence (CAT) or a critical level, where the intrinsic frequency vanishes, waves propagate vertically upward to the a great vertical distance. Lilly (1972)[9] reported the value of the momentum flux over the Front Range of the Colorado Rockies by instrumented aircraft during field experiments.

Bluemen and McGergor (1976)[10] had studied the effect of both cross wind and vertical shear of the basic flow in a linear, hydrostatic model of stationary mountain lee waves in a stably stratified air stream. Using a constant lapse rate basic flow, analytical solutions were determined first. They compared the solution for the basic flow (U = sechy) with that for the constant basic flow (U= constant). They introduced a 3-D mountain wave drag model for a non-planar shear flow. They observed the wave drag obtained by 2-D barrier was greater than that obtained by a 3-D barrier. In their study they had also taken a two layer model in order to examine the effect of stable stratosphere. In this study the wave drag was shown to be sensitive to the phase difference between the transmitted and reflected waves in the lower layer. They found that this sensitiveness becomes more pronounced in the presence of crosswind shear.

Andrews and Mclntyre (1976)[11] had shown that finite

amplitude waves transfer momentum to the mean flow only when they are transient or dissipative. The pressure drag on the Blue Ridge mountain in the central Appalachians was determined by Smith (1978)[12]. He observed during the first two weeks of January 1947 several periods with important wave drag with pressure differences typically of the order of $50Nm^{-2}$ across the ridge. The general westerly bias (GWB) of the global GCM (general circulation models) were developed by Palmer et al. (1986)[13]. They also observed that one way to reduce this GWB is to incorporate the gravity wave drag parameterization scheme in the GCM. They used a straightforward zonally symmetric model demonstrates the mechanisms through which adjustments to thermal wind balance, combined with wave drag in the stratosphere, lead to warming in polar areas through adiabatic descent, while simultaneously slowing down the average westerly winds in the troposphere. They discussed the impact of the parameterization scheme on simulations within the 11-layer model and found it to be largely advantageous for the integrations.

Iwasaki et al. (1989)[14] developed an another type of gravity wave drag parameterization scheme to upgrade the troposphere westerly bias associated with effects of these tropospheric trapped lee waves. Hoinka and Clark (1991)[15] had used a 3-D, anelastic and no-hydrostatic model to simulate the airflow over and around Alps during a strong foehn event on 8th November 1982. Their model results showed that in low levels the airflow is moved around Alps. They also observed that, the local vectors of the momentum flux and the pressure drag exhibit notable horizontal fluctuation, according to the simulations. This variability limits the capacity to reliably extrapolate local cross-sectional observations of pressure drag and momentum flux to values representative for the entire Alpine complex and makes it more difficult to compare model and observational data. Unfortunately, on November 8, 1982, surface pressure drag readings for the entire Alps were not available. Clark and Miller (1991)[16] again presented a 3-D nested non-hydrostatic model across ALPEX. They also showed that the variability of the momentum fluxes. Satomura and Bougeault (1994)[17] used a two dimensional non-hydrostatic, compressible model to simulate the airflow over the Pyrenees in connection with two lee waves events during PYREX experiment. In both cases, the simulated downward momentum fluxes agree well with the observed fluxes around 4km height. The over estimation of the simulated momentum flux in the upper half of the atmosphere was suggested to be due to the time evolution of the mean wind and the lateral momentum flux divergence found in the atmosphere.

Shutts (1995)[18] was analytically demonstrated that, except for the azimuthal filtering, the momentum flux vector for an environmental flow with a uniform shear is almost the same as that for a uniform environmental flow, where velocity is equal to the original flow at the ground level. Broad (1995)[19] developed a 3-D linear theory of momentum fluxes associated with turning of the mean wind with height. He showed that unless the Richardson number drops below a quarter or there is a critical level where the mean wind in the direction of the flux vector becomes zero, the vertical flux of the horizontal momentum vector is thought to be parallel to the surface stress vector and independent of height. Then, non-zero gravity-wave drag is assumed to be opposed to the flow vector and parallel to it. Shutts (1998)[20] developed a 3-D linear theory of momentum fluxes. He viewed that the flux is azimuthally filtered continuously in the vertical. Vosper and Mobbs (1998)[21] also considered a 3-D dynamical model for momentum fluxes for a steady waves. They observed that the horizontal components of momentum flux are constant with height in the nonappearance of dissipation.

Dutta (2001)[22] contemplated a 2-D bell shaped model for an idealized air-stream flow across Mumbai-Pune section of the Western Ghats (WG). He observed that both fluxes (momentum and energy fluxes) are fixed with height and have no contribute of plateau part of the barrier to the aforesaid fluxes. Dutta and Naresh Kumar (2005)[23] also developed a 2-D flux model across the Assam-Burma Hills (ABH). They displayed that the valley of ABH acts as a source and sink in the momentum flux and energy flux respectively. Dutta (2007)[24] modified his 2-D model into 3-D realistic model across WG and KJH. He showed that the momentum all the fluxes across both Western-Ghats (WG) and KJH are varying with vertical but vertical variation is not uniform with height. He also observed the influence of V component of the basic flow, this component makes the momentum flux or energy flux either divergent or convergent in the vertical. Das and Dutta (2022)[25] developed a mathematical model on fluxes associated with gravity waves excited by corner mountain. The observed the effect of the corner mountain which is formed by ABH and KJH and showed that the fluxes

are varying with vertical but variations are not uniform with height.

There appears to be limited research on momentum and energy flux associated with internal gravity waves generated by the Assam-Burma Hills and Khasi-Jaintia Hills (KJH), especially considering the actual vertical patterns of background wind and stability. With this brief discussion we pass on to the development of this mathematical model for both fluxes associated with gravity wave in different atmospheric phenomena over northeast region of India.

2. Database

The nearest RS (Radio Sonde) station to both Khasi-Jayantia Hills (KJH) and Assam-Burma Hills (ABH) of northeast region of India is GUWAHATI (26.19°N, 91.73°E). The average observed lee waves RS data of GUWAHATI for 26th January 2020 from 0000UTC to 1200UTC across the barriers of northeast region of India, have been used in this study. This data is taken from Archive of IMD (Indian Meteorological Department), Pune, India.

3. Methodology

In the northeast region of India, the Khasi-Jaintia Hills (KJH) and Assam-Burma Hills (ABH) are two important mountain barriers serving as study profiles for this model. KJH is broadly eastwest oriented whereas ABH is broadly northsouth oriented and ABH is synthesized by two elliptical barriers they are separated by a valley of some finite length. The analytical expressions of these two profiles are:

Profile of KJH (Dutta (2007)[24]):

$$h(x,y) = \frac{H}{1+\frac{x^2}{a^2}+\frac{y^2}{b^2}} \tag{1}$$

Profile of ABH (Das et al. (2018)[26]):

$$h(x,y) = \frac{h_1}{1+\frac{x^2}{a^2}+\frac{y^2}{b^2}} + \frac{h_2}{1+\frac{(x-d)^2}{a^2}+\frac{y^2}{b^2}} \tag{2}$$

The meaning of all parameters of the above profiles are given in **Table 1**[24,26].

We assume the KJH to be a single elliptical barrier and the ABH to be two elliptical barriers, separated by a valley of finite length (d). The major ridge of the barrier is normal to the basic flow. A laminar, steady state, inviscid, non-rotating and adiabatic baroclinic mean flow is taken in this model. Both components V and U of basic flow and the Brunt-Väisälä frequency (N) are varying with vertical. Using the same conditions and same method of Das and Dutta (2022)[25], we get a vertical structure equation:

Table 1. Meaning and Values of the Parameters of the Barrier.

Barriers	Meaning and Values of the Parameters
KJH	a = half the width of the barrier along the basic flow =25km b = half the width of the barrier across the basic flow=62.5km H=Height of the Ridge =1.6km
ABH	a = half the width of the barrier along the basic flow =20km b = half the width of the barrier across the basic flow=50km h_1=Height of the 1st Ridge =0.9km h_2=Height of the 2nd Ridge =0.7km d =Length of the valley between two Ridges.

$$\frac{\partial^2 \widehat{w_1}}{\partial z^2} + \left\{ f(k,l,z) - K^2 \right\} \widehat{w_1} = 0 \tag{3}$$

$$f(k,l,z) = \frac{N^2(k^2+l^2)}{(kU+lV)^2} - \left(\frac{k\frac{dU}{dz} + l\frac{dV}{dz}}{ku+lV} \right) \frac{1}{\rho_0}\frac{d\rho_0}{dz} - \left(\frac{k\frac{d^2U}{dz^2} + l\frac{d^2V}{dz^2}}{ku+lV} \right) + \frac{1}{4\rho_0^2}\left(\frac{d\rho_0}{dz}\right)^2 - \frac{1}{2\rho_0}\frac{d^2\rho_0}{dz^2} \tag{4}$$

where $\acute{w}(x,y,z) = \sqrt{\frac{\rho_0(0)}{\rho_0(z)}} w_1(x,y,z)$, $N = \sqrt{\frac{g}{\theta_0}\frac{d\theta_0}{dz}}$ and $K^2 = k^2 + l^2$. All other symbols have the same meaning of Das and Dutta (2022)[25]. Numerical solution of equation (3) is strictly indeterminate unless the value of $f(k,l,z)$ is specified at great heights. But, it is physically unlikely that the computed flow pattern at the lower levels would be greatly affected by the temperature and at the great height. Also Corby and Sawyar (1958)[8], Palm and Foldvic (1960)[27] and Sawyar (1960)[28] have observed that the choice of $f(k,l,z)$ at the upper boundary has only a small effect on low-level flow patter. Accordingly it is considered here that, at and above the upper boundary $f(k,l,z) = 0$, Viz., Sarker (1967)[29], De (1973)[30], Sinha Ray (1988)[31]. Thus at and above the upper boundary condition we have

$$\widehat{w_1}(k,l,z) \propto e^{-Kz} \tag{5}$$

$$\frac{\partial \widehat{w_1}}{\partial z} \propto -K\widehat{w_1} \tag{6}$$

If $\widehat{h}(k,l)$ be the 2-D Fourier transformation of $h(x,y)$. Then the Fourier transformations of the profiles (1) and (2) are

$$\widehat{h}(k,l) = 2\pi abH K_0\left(a^2k^2 + b^2l^2\right) \tag{7}$$

$$\widehat{h}(k,l) = 2\pi ab\left(h_1 + h_2 e^{-ikd}\right) K_0\left(a^2k^2 + b^2l^2\right) \tag{8}$$

For the numerical solutions, following Das and Dutta (2022)[25], we consider an arbitrary function $\phi(k,l,z)$ that satisfies equation (3) and boundary conditions (5) and (6). Using the same technique and procedure of Das and Dutta (2022)[25], the solution of equation (3) is expressed as

$$\widehat{w}(k,l,z) = \sqrt{\frac{\rho_0(0)}{\rho_0(z)}} i\left[kU(0) + lV(0)\right]\widehat{h}(k,l)\frac{\varphi(k,l,z)}{\varphi(k,l,0)} \tag{9}$$

Where $\widehat{h}(k,l)$ for KJH and ABH are given by equations (7) and (8) respectively. Now numerical solution of $\phi(k,l,z)$ is calculated at discrete levels in the vertical for a given pair of wave number (k,l). So, the model domain is artificially divided vertically in n discrete levels by inserting (n+1) equidistant (d) points. For a given pair of wave number is specified at each of the (n+1) discrete levels, obtained from RS (radio sonde) data for upstream station of the barrier. Now, similar to Das and Dutta (2022)[25], $\phi(k,l,z)$ is calculated numerically at different vertical grid points at intervals of 0.25 km and at different levels, for a given vector (k,l). Using (9) and the values of $\phi(k,l,z)$, we calculate $\widehat{p}$, $\widehat{u}$ and $\widehat{v}$ {following Das and Dutta (2022)[25], Dutta (2005)[32], Dutta (2007)[24]}

$$\widehat{p}(k,l,z) = \frac{i\left\{\left(k\frac{dU}{dz} + l\frac{dV}{dz}\right)\widehat{w}(k,l,z) - (kU + lV)\frac{\partial \widehat{w}}{\partial z}\right\}\rho_0(z)}{K^2} \tag{10}$$

$$\widehat{u}(k,l,z) = \frac{i\left[\widehat{w}(k,l,z)\frac{dU}{dz} + \frac{k}{K^2}\left\{\left(k\frac{dU}{dz} + l\frac{dV}{dz}\right)\widehat{w}(k,l,z) - (kU + lV)\frac{\partial \widehat{w}}{\partial z}\right\}\right]}{(kU + lV)} \tag{11}$$

$$\widehat{v}(k,l,z) = \frac{i\left[\widehat{w}(k,l,z)\frac{dV}{dz} + \frac{k}{K^2}\left\{\left(k\frac{dU}{dz} + l\frac{dV}{dz}\right)\widehat{w}(k,l,z) - (kU + lV)\frac{\partial \widehat{w}}{\partial z}\right\}\right]}{(kU + lV)} \tag{12}$$

Applying inverse Fourier transformation on equations (9)-(12) numerically, w', p', u' and v' are calculated at each vertical level and at each horizontal grid point (5km apart). Similar to Das and Dutta (2022)[25], the two horizontal components of the momentum flux vector $T_{zx} = Su'w'$, $T_{zy} = Sv'w'$ and energy flux $E_z = Sp'w'$ at horizontal grid point and any vertical level and any horizontal grid, are computed. Where S denotes the average surface area of the given barrier. Here the average surface area of the barrier KJH is $S_{KJH} = 0.5\pi^2(a+b)H$ as per equation (1) [Dutta (2007)[24]] and for the barrier ABH is $S_{ABH} = 0.5(h_1 + h_2)\{\pi^2(a+b) + d\}$ as per equation (2) [Das et al. (2016)[33]].

4. Results and Discussion

Applying the equations (10)-(12), the fluxes have been calculated across the barriers KJH and ABH. The duration from November to February, is the winter season for the India subcontinent. Das et al. (2016)[33], Dutta and Naresh Kumar (2005)[23] and De (1973)[30] had marked that the air stream occurs the lee waves during this winter season across the KJH and ABH. So, in this study, we take a particular date 26th January 2020. This date is known to every Indian as the Republic day and they celebrate this day in every year. Here, the computed energy fluxes and momentum fluxes are discussed with respect to KJH and ABH separately below.

4.1. Fluxes for KJH during Winter Season (On 26th January 2020)

In the northeast region of India, the Khasi-Jaintia Hills (KJH) is a crucial mountain barrier that plays a significant role in exciting gravity waves associated with 3-D mesoscale airflow. The vertical profile of temperature T(z) and two parts U(z) and V(z) of the basic flow are graphed by the **Figure 1**. This shows that the U(z) and V(z) are changing with vertical and the temperature T(z) is constant moist adiabatic lapse rate with height. Using this profile, the energy flux (E_{kjh}) and momentum fluxes (T_{zx_kjh} , T_{zy_kjh}) are obtained across the barrier KJH.

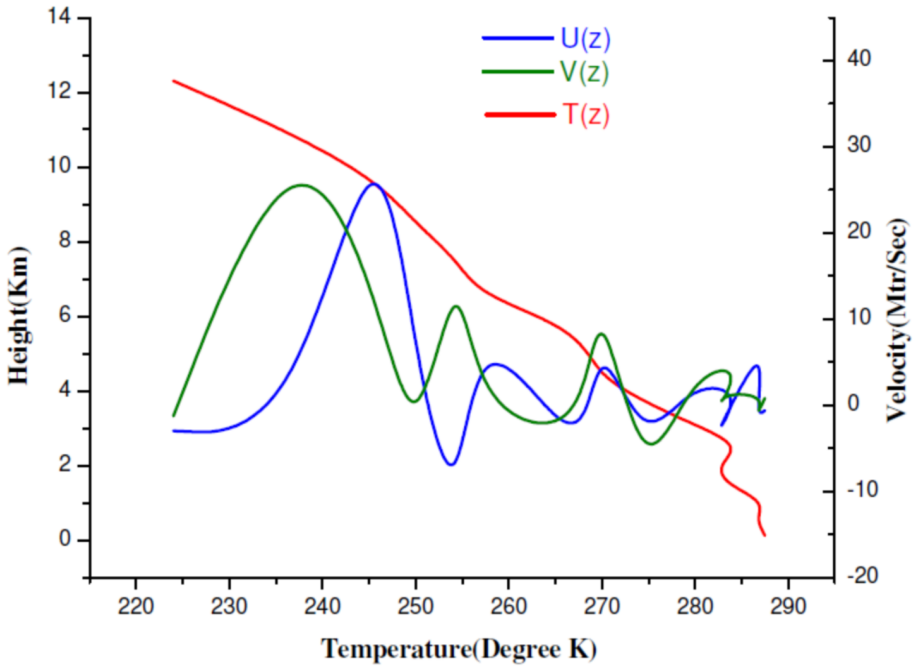

Figure 1. Vertical profile of T(z), U(z) and V(z).

The energy flux (E_{kjh}) across KJH on 26th January 2020 is shown in **Figure 2**. This figure shows that the energy flux is unchanged above 3.25 km and variant from ground level to 3.25 km. When z = 1.25 km, there is a maximum energy flux E_{kjh} has been found and in the level from z = 0.5 km to z = 1.75 km, E_{kjh} is vertically upward. In the level from z = 1.75 km to z = 3.25 km, E_{kjh} is vertically downward. The magnitude of the maximum energy flux E_{kjh} at z = 1.25 km, is $2.53E-04W(msq)^{-1}$.

The profile of westerly momentum flux (T_{zx_kjh}) is depicted in the **Figure 3**. The momentum flux T_{zx_kjh} is unchanged above z = 3.5 km and in the level from z = 0.5 km to z = 1.75 km, T_{zx_kjh} is vertically upward and from z = 1.75 km to z = 3.5 km, T_{zx_kjh} is upward/downward. The maximum momentum flux T_{zx_kjh} at z = 1.25 km is found and its magnitude is $1.07E-10N(msq)^{-1}$.

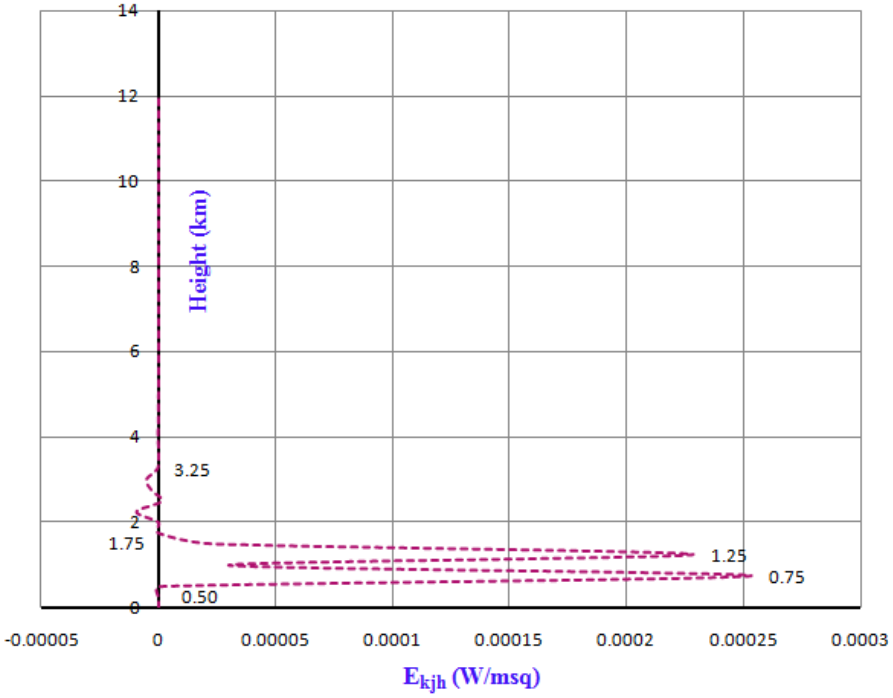

Figure 2. Vertical profile of Energy flux (E_{kjh}) for KJH.

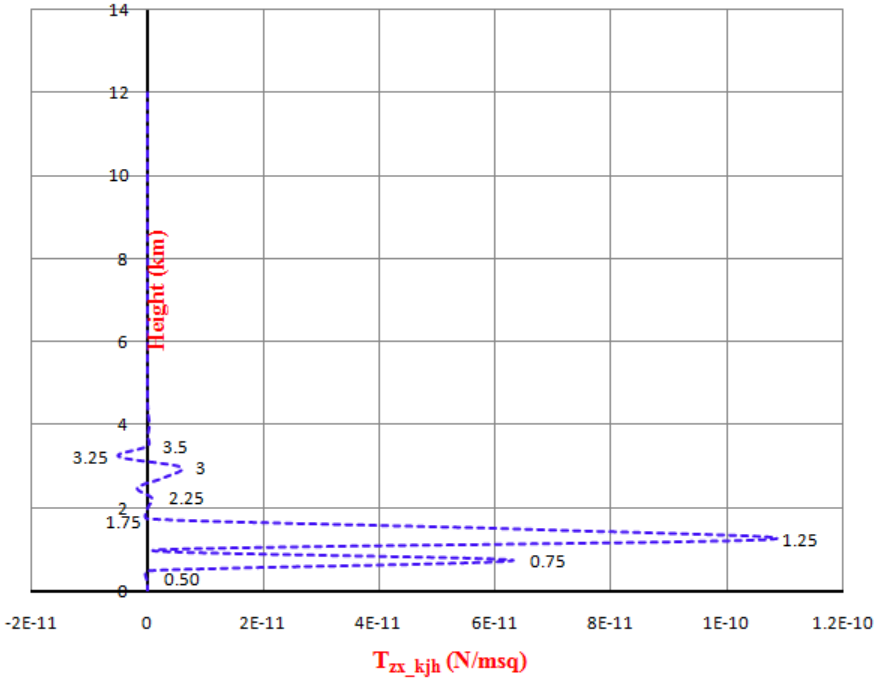

Figure 3. Vertical profile of Momentum flux (T_{zx_kjh}) for KJH.

The profile of southerly momentum flux (T_{zy_kjh}) across KJH is graphed in the **Figure 4**. In the level from z = 0.5 km to z = 1 km and from z = 1 km to z = 1.75 km, the flux T_{zy_kjh} is vertically upward and downward respectively. It is marked that, in the level from z = 0.5 km to z = 4.25 km the southerly momentum flux (T_{zy_kjh}) is divergent/convergent and it is unchanged above z = 4.25 km and the maximum flux T_{zy_kjh} occurs at z = 1.5 km with magnitude $|-2.19E-11|N(msq)^{-1}$.

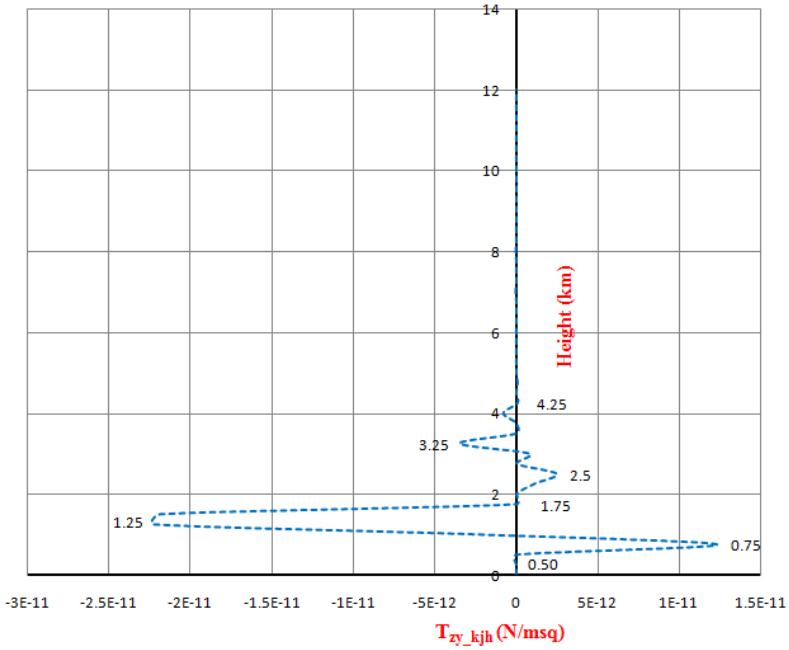

Figure 4. Vertical profile of Momentum flux (T_{zy_kjh}) for KJH.

4.2. Fluxes for ABH during Winter Season (On 26th January 2020)

ABH is synthesized by two ridges separated by a valley of some finite length (d). The weather and climate of the northeast region of India depend on the behaviour of the ABH. Using the same profile of T(z), U(z) and V(z), the fluxes are calculated across the barrier ABH.

The energy flux (E_{abh}) across ABH is depicted in the **Figure 5**. It is shown that the energy flux E_{abh} is fixed above z = 3.5 km. In the level from z = 0.5 km to z = 1.75 km the flux E_{abh} is vertically upward and from z = 1.75 km to z = 3.5 km the flux E_{abh} is vertically downward i.e., the flux E_{abh} is convergent/divergent up to z = 3.5 km. The maximum energy flux E_{abh} is seen at z = 1.25km and its magnitude is $5.28E-04W(msq)^{-1}$.

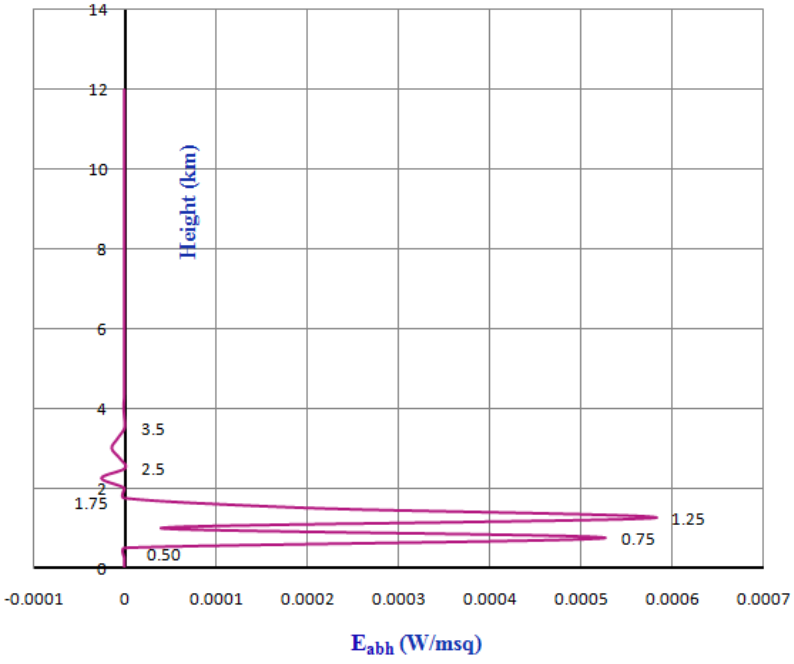

Figure 5. Vertical profile of Energy flux (E_{abh}) for ABH.

The profile of the westerly momentum flux (T_{zx_abh}) across ABH is shown in **Figure 6**. This shows that the maximum momentum flux is occurred at z = 1.25 km and its value is $2.23E-10N(msq)^{-1}$. In the level from z = 0.5 km to z = 1.75 km, the momentum flux T_{zx_abh} is vertically upward and also it is invariant above z = 3.5 km.

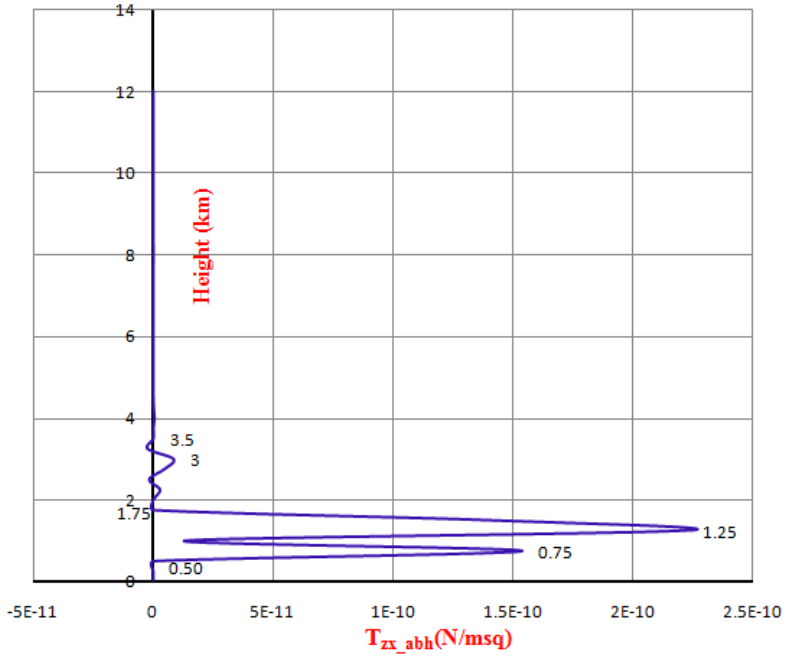

Figure 6. Vertical profile of Momentum flux (T_{zx_abh}) for ABH.

The profile of the southerly momentum flux (T_{zy_abh}) across ABH is depicted in **Figure 7**. In the lavel from z = 0.5 km to z = 1 km and from z = 1 km to z = 1.75 km, the momentum flux T_{zy_abh} is vertically upward and downward respectively. Again from z = 1.75 km to z = 4.25 km, the flux T_{zy_abh} is vertically upward/downward and invariant above z = 4.25 km. The maximum southerly momentum flux T_{zy_abh} occurs at z = 4.25 km and its magnitude is $4.05E-11N(msq)^{-1}$.

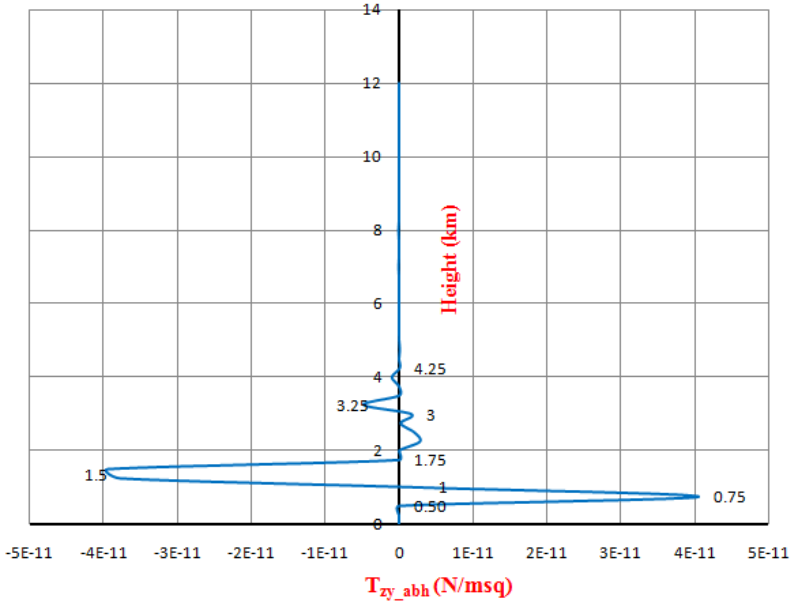

Figure 7. Vertical profile of Momentum flux (T_{zy_abh}) for ABH.

5. Conclusions

In this work, we calculate and parameterize the fluxes associated with airflow over the northeast region of India. The results reveal several notable observations, which are presented below:

(i) In the northeast region of India, the maximum energy fluxes of the barriers are occurred near about at z = 1.25 km and the energy fluxes across both KJH and ABH are vertically upward from ground level to z = 2 km.

(ii) The maximum westerly momentum fluxes across both KJH and ABH are located at z = 1.25 km and these westerly momentum fluxes are vertically upward from ground level to z = 1.75 km.

(iii) The southerly momentum fluxes across both the barriers are vertically upward and downward in the level from surface to z = 2 km and the maximum southerly momentum fluxes are located at z = 1.5 km.

(iv) The effects of the barriers of northeast region of India are observed and they are playing a major roll to create energy flux and momentum flux.

The climate and weather of the northeast region of India are observed to depend on the orographic behaviour of the KJH and ABH barriers.

Funding

This research work was completed without any external funding.

Institutional Review Board Statement

Not applicable.

Informed Consent Statement

Not applicable.

Data Availability Statement

Data was collected from IMD (India Meteorological Department), Pune, India.

Acknowledgments

The author is grateful to Dr. U.S. De, Former Additional. Director General of Meteorology of India Meteorological Department (IMD) and to Dr. S. Dutta, Scientist-G and DDGM-SECRETARIAT, RMC Kolkata and to Prof. M. Maiti, Retd. Professor and Prof. Shyamal Kumar Mandal, Dept. of Applied Mathematics, VU, Midnapore, W.B., India and Dr. Ranjan Kumar Jana, Department of Mathematics and Associate Dean (Academic), Sardar Vallabhbhai National Institute of Technology, Surut-395007, Gujrat, India for their valuable suggestions and guidance. The author acknowledge the use of Fortran-77 for data programming, Microsoft office Excel and Origin for drawing graph. We also appreciate the comments of the anonymous reviewers which helped to improve the quality of the manuscript.

Conflicts of Interest

The author declares no conflict of interest.

References

[1] Corby, G.A., Sawyer, J.S., 1958. The air flow over a ridge-the effects of the upper boundary and high-level conditions. Quarterly Journal of the Royal Meteorological Society. 84(359), 25–37. DOI: https://doi.org/10.1002/qj.49708435904

[2] Sawyer, J.S., 1959. The introduction of the effects of topography into methods of numerical forecasting. Quarterly Journal of the Royal Meteorological Society. 85(363), 31–43. DOI: https://doi.org/10.1002/qj.49708536304

[3] Eliassen, A., Palm, E., 1961. On the transfer of energy in stationary mountain waves. Geofysiske Publikasjoner. 22, 1–23.

[4] Sawyar, J.S., 1962. Gravity waves in the atmosphere as a three-dimensional problem. Quarterly Journal of the Royal Meteorological Society. 88, 412–425. DOI: https://doi.org/10.1002/qj.49708837805

[5] Blumen, W., 1965. A random model of momentum flux by mountain waves. Geofysiske Publikasjoner. 26(2), 33.

[6] Booker, J.R., Bretherton, F.P., 1967. The critical layer for internal gravity waves in a shear flow. Journal of fluid mechanics. 27(3), 513–539. DOI: https://doi.org/10.1017/S0022112067000515

[7] Miles, J.W., 1968. Lee waves in a stratified flow

Part 1. Thin barrier. Journal of Fluid Mechanics. 32(3), 549–567. DOI: https://doi.org/10.1017/S0022112068000893

[8] Bretherton, F.P., 1969. Momentum transport by gravity waves. Quarterly Journal of the Royal Meteorological Society. 95(404), 213–243. DOI: https://doi.org/10.1002/qj.49709540402

[9] Lilly, D.K., 1972. Wave momentum flux-A GARP problem. Bulletin of the American Meteorological Society. 53(1), 17–24. DOI: https://doi.org/10.1175/1520-0477-53.1.17

[10] Blumen, W., McGregor, C.D., 1976. Wave drag by three-dimensional mountain lee-waves in nonplanar shear flow. Tellus. 28(4), 287–298. DOI: https://doi.org/10.3402/tellusa.v28i4.10295

[11] Andrews, D.G., Mcintyre, M.E., 1976. Planetary waves in horizontal and vertical shear: The generalized Eliassen-Palm relation and the mean zonal acceleration. Journal of Atmospheric Sciences. 33(11), 2031–2048. DOI: https://doi.org/10.1175/1520-0469(1976)033<2031:PWIHAV>2.0.CO;2

[12] Smith, R.B., 1978. A measurement of mountain drag. Journal of Atmospheric Sciences. 35(9), 1644–1654. DOI: https://doi.org/10.1175/1520-0469(1978)035<1644:AMOMD>2.0.CO;2

[13] Palmer, T.N., Shutts, G.J., Swinbank, R., 1986. Alleviation of a systematic westerly bias in general circulation and numerical weather prediction models through an orographic gravity wave drag parametrization. Quarterly Journal of the Royal Meteorological Society. 112(474), 1001–1039. DOI: https://doi.org/10.1002/qj.49711247406

[14] Iwasaki, T., Yamada, S., Tada, K., 1989. A parameterization scheme of orographic gravity wave drag with two different vertical partitionings part I: Impacts on Medium-range forecasts. Journal of the Meteorological Society of Japan. Ser. II. 67(1), 11–27. DOI: https://doi.org/10.2151/jmsj1965.67.1_11

[15] Hoinka, K.P., Clark, T.L., 1991. Pressure drag and momentum fluxes due to the Alps. I: Comparison between numerical simulations and observations. Quarterly Journal of the Royal Meteorological Society. 117(499), 495–525. DOI: https://doi.org/10.1002/qj.49711749905

[16] Clark, T.L., Miller, M.J., 1991. Pressure drag and momentum fluxes due to the Alps. II: Representation in large-scale atmospheric models. Quarterly Journal of the Royal Meteorological Society. 117(499), 527–552. DOI: https://doi.org/10.1002/qj.49711749906

[17] Satomura, T., Bougeault, P., 1994. Numerical simulation of lee wave events over the Pyrenees. Journal of the Meteorological Society of Japan. Ser. II. 72(2), 173–195. DOI: https://doi.org/10.2151/JMSJ1965.72.2_173

[18] Shutts, G.J., 1995. Gravity-wave drag parametrization over complex terrain: The effect of critical-level absorption in directional wind-shear. Quarterly Journal of the Royal Meteorological Society. 121(525), 1005–1021. DOI: https://doi.org/10.1002/qj.49712152504

[19] Broad, A.S., 1995. Linear theory of momentum fluxes in 3-D flows with turning of the mean wind with height. Quarterly Journal of the Royal Meteorological Society. 121(528), 1891–1902. DOI: https://doi.org/10.1002/qj.49712152806

[20] Shutts, G.J., 1998. Stationary gravity-wave structure in flows with directional wind shear. Quarterly Journal of the Royal Meteorological Society. 124(549), 1421–1442. DOI: https://doi.org/10.1002/qj.49712454905

[21] Vosper, S.B., Mobbs, S.D., 1998. Momentum fluxes due to three-dimensional gravity-waves: Implications for measurements and numerical modelling. Quarterly Journal of the Royal Meteorological Society. 124(552), 2755–2769. DOI: https://doi.org/10.1002/qj.49712455211

[22] Dutta, S., 2001. Momentum flux, energy flux and pressure drag associated with mountain wave across western ghat. Mausam. 52(2), 325–332. DOI: https://doi.org/10.54302/mausam.v52i2.1699

[23] Dutta, S., Naresh, K., 2005. Parameterization of momentum and energy flux associated with mountain wave across the Assam-Burma hills. Mausam. 56(3), 527–534. DOI: https://doi.org/10.54302/mausam.v56i3.980

[24] Dutta, S., 2007. Parameterization of momentum flux and energy flux associated with orographically excited internal gravity waves in a baroclinic background flow. Mausam. 58(4), 459–470. DOI: https://doi.org/10.54302/mausam.v58i4.1373

[25] Das, P., Dutta, S., 2022. A mathematical model for fluxes associated with internal gravity waves excited by a corner mountain. Mausam. 73(1), 181–188. DOI: https://doi.org/10.54302/mausam.v73i1.5091

[26] Das, P., Dutta, S., Mondal, S.K., 2018. A dynamical model for diagnosing orographic rainfall across Assam–Burma hills in India. Modeling Earth Systems and Environment. 4(4), 1423–1433. DOI: https://doi.org/10.1007/s40808-018-0492-3

[27] Palm, E., Foldvik, A., 1960. Contribution to the theory of two-dimensional mountain waves. Aschehoug: Oslo, Norway.

[28] Sawyer, J.S., 1960. Numerical calculation of the displacements of a stratified airstream crossing a ridge of small height. Quarterly Journal of the Royal Meteorological Society. 86(369), 326–345. DOI: https://doi.org/10.1002/qj.49708636905

[29] Sarker, R.P., 1967. Some modifications in a dynamical model of orographic rainfall. Monthly weather review. 95(10), 673–684. DOI: https://doi.org/10.1175/

1520-0493(1967)095<0673:SMIADM>2.3.CO;2

[30] De, U.S., 1973. Some studies on mountain waves [PhD Thesis]. Banaras Hindu University: Varanasi, India.

[31] Sinha Ray, K.C., 1988. Some studies on effects of Orography on airflow and rainfall [PhD Thesis]. University of Pune: Pune, India.

[32] Dutta, S., 2005. Effect of static stability on the pattern of three-dimensional baroclinic lee wave across a meso scale elliptical barrier. Meteorology and Atmospheric Physics. 90(3), 139–152. DOI: https://doi.org/10.1007/s00703-004-0086-7

[33] Das, P., Dutta, S., Mondal, S.K., et al., 2016. Momentum flux and energy flux associated with internal gravity waves excited by the Assam-Burma hills in India. Modeling Earth Systems and Environment. 2, 1–9. DOI: https://doi.org/10.1007/s40808-016-0118-6